

Review

# Metal–Organic Framework (MOF)-Derived Catalyst for Oxygen Reduction Reaction (ORR) Applications in Fuel Cell Systems: A Review of Current Advancements and Perspectives

Karmegam Dhanabalan <sup>1,\*</sup>, Muthukumar Perumalsamy <sup>2</sup>, Ganesan Sriram <sup>1</sup>, Nagaraj Murugan <sup>3</sup>, Shalu <sup>4</sup>, Thangarasu Sadhasivam <sup>1,\*</sup> and Tae Hwan Oh <sup>1,\*</sup>

<sup>1</sup> School of Chemical Engineering, Yeungnam University, Gyeongsan 38541, Republic of Korea; sriram2085@gmail.com

<sup>2</sup> Nanomaterials & System Laboratory, Major of Mechatronics Engineering, Faculty of Applied Energy System, Jeju National University, Jeju 63243, Republic of Korea; muthuku20@gmail.com

<sup>3</sup> Department of Polymer Engineering, Graduate School, School of Polymer Science and Engineering & Alan G. MacDiarmid Energy Research Institute, Chonnam National University, Yongbong-ro, Buk-gu, Gwangju 61186, Republic of Korea; n.muruganp@gmail.com

<sup>4</sup> Department of Physics, School of Basic Sciences and Research, Sharda University, Greater Noida 201310, India; shalu.kataria9@gmail.com

\* Correspondence: dhanabalan\_nano@yahoo.co.in (K.D.); sadhasivam.nano@gmail.com (T.S.); taehwanoh@ynu.ac.kr (T.H.O.)

**Abstract:** High-porosity, crystalline, and surface-area-rich metal–organic frameworks (MOFs) may be employed in electrochemical energy applications for active catalysis. MOFs have recently been modified using secondary building blocks, open metal sites with large pore diameters, and functional ligands for electronic conductivity. They have the potential for excellent performance in fuel cell applications, and they have several possibilities to enhance the fundamental characteristics of mass and electron transportation. MOFs may be combined with other materials, such as solitary metal nanoparticles and carbon and nitrogen composites, to increase their catalytic efficacy, especially in oxygen reduction reaction (ORR). As a result, this study focuses on MOF derivatives for ORR applications, including porous carbon MOF, single metal MOF-derived composites, metal oxides, and metal phosphides. An efficient MOF electrocatalyst platform for ORR applications is presented, along with its prospects. These initiatives promote promising MOF electrocatalysts for enhancing fuel cell efficiency and pique curiosity for possible growth in subsequent research.

**Keywords:** metal–organic framework; electrocatalyst; nanoparticles; oxygen reduction reaction; fuel cell



**Citation:** Dhanabalan, K.; Perumalsamy, M.; Sriram, G.; Murugan, N.; Shalu; Sadhasivam, T.; Oh, T.H. Metal–Organic Framework (MOF)-Derived Catalyst for Oxygen Reduction Reaction (ORR) Applications in Fuel Cell Systems: A Review of Current Advancements and Perspectives. *Energies* **2023**, *16*, 4950. <https://doi.org/10.3390/en16134950>

Academic Editor: Giuseppe Bagnato

Received: 22 May 2023

Revised: 22 June 2023

Accepted: 23 June 2023

Published: 26 June 2023



**Copyright:** © 2023 by the authors. Licensee MDPI, Basel, Switzerland. This article is an open access article distributed under the terms and conditions of the Creative Commons Attribution (CC BY) license (<https://creativecommons.org/licenses/by/4.0/>).

## 1. Introduction

Using non-renewable energy sources, such as fossil fuels, necessitates the development of green energy technology to prevent environmental damage [1]. As a result of the deterioration of the environment and the insufficiency of energy resources, it is becoming ever more important to develop more modern methods of energy production [2]. Generation of electricity from sources of a smaller scale is proposed, with the primary goal being an increase in output of renewable energy sources [3]. Other than energy devices, the fuel cell may convert energy efficiently and sustainably. Fuel cells, a method of converting energy, might utilize hydrogen and several other fuels [4]. An anode and a cathode are both parts of the fuel cell, and they are physically separated by a proton exchange membrane (PEM) [5]. Proton exchange membrane fuel cells (PEMFCs) are an environmentally beneficial alternative to fossil fuels for energy conversion [6]. However, the use of PEMFCs has been limited due to insufficient resources and the expensive cost of the platinum (Pt) catalyst for the oxygen reduction reaction (ORR) [7]. The higher d-orbital vacant sites have facilitated the

selective charge carriers during the anodic and cathodic reactions. However, one of the important half-reactions in PEMFCs, which may convert energy effectively and sustainably, is poor durability, greater cross-over phenomena, and an ORR at the cathode [8]. Therefore, research is required to develop ORR catalysts to reduce the cost-effective energy conservation of PEMFCs. The platinum group free metals and metal oxides for electrocatalysts have been the subject of much investigation [9]. Certain metal oxides, however, have limited long-term stability and low conductivity [10]. For diverse electrocatalytic applications, heteroatom-doped (N and S) and conductive porous carbon-embedded metal and metal oxide are developed to maximize conductivity [11,12]. On the other hand, these are not characteristics that make one hopeful about the ORR response in the PEMFCs. As a result, researchers are concentrating their efforts on three-dimensional hollow structures to increase crystallinity qualities, low density, large surface area, and low mass [13]. The above materials are produced by pyrolysis for metal-doped carbon precursors with heteroatom incorporation [14]. In the 1990s, researchers invented a metal–organic framework with exceptional electrocatalytic properties. MOFs have garnered considerable interest as ORR candidates. Due to their composition, pore size, and hierarchy, they appear to be highly adaptable [15].

Crystalline porous materials are porous coordination polymers (PCPs) and metal–organic frameworks (MOFs). They consist of metal ions and clusters held together by organic ligands through coordination bonds known as secondary building units (SBUs). Producing MOFs with varied surface functions, particle morphologies, and pore structures may be achieved easily using an infinite number of combinations of inorganic and organic components. MOFs have lately become more prominent in the research field of fuel cell applications. [16]. However, pure MOFs have significant drawbacks in their properties, such as low stability and poor electrical conductivity for applications. Therefore, carbon-based MOFs derived from precursors of oxides, carbides, phosphides, and chalcogenides offer a variety of nanomaterials with highly permeable surface morphologies [17]. MOF metal- and carbon-based nanostructured components create numerous porous structures, including metal clusters, ions, and organic linkages [18]. Recently, MOFs have drawn much interest in nanoporous carbons (NPCs) as innovative templates for developing NPCs. It is possible to produce NPCs with direct carbonization of MOFs without any extra precursors. MOFs contain a significant amount of carbon in their structures. During their analysis, MOFs evolve into a distinctive NPC material that contains their clearly defined precursors with a large surface area and big holes. Most metal oxide-based MOFs demonstrated prominent characteristics such as hydrophobic surfaces, large surface areas, and varied pore sizes [19]. The complementary features of both categories of functional elements are advantageous for metal oxides produced from MOFs. They function well as catalysts and conductors, and the structural features of the MOF materials may be preserved. This article also looks at the development processes for MOFs, their intrinsic and extrinsic characteristics, and their applications, particularly for the ORR in PEMFCs. We believe that future researchers will be encouraged to investigate MOF composites for ORR application in PEMFCs due to the data, usage, and functionality in detail in this study. The key points of this review are briefly described in Figure 1. Recent reviews on MOF-based nanomaterials from 2018 are ORR applications and cutting-edge MOF-derived electrocatalysts for fuel cell applications.

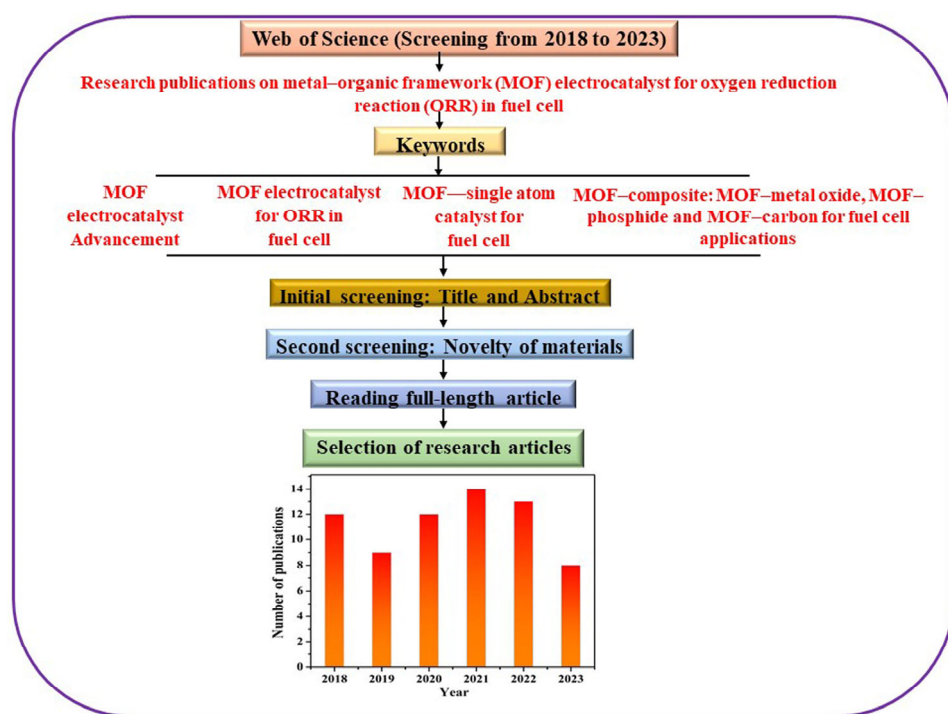


**Figure 1.** A schematic depiction of the criteria considered while selecting research papers from Web of Science from 2018 to the present for this review.

## 2. A MOF-Based Conceptual Highlight

MOFs are effective as catalysts. With various metal ions or clusters, organic linkages, and a rapid manufacturing process, MOFs promise to make more complex catalysts. As catalysts for ORR applications, MOFs are promising [20]. The simple carbonization procedure produces a functional metal with a large surface area and a heteroatomic doping effect. MOF materials can be made with organic links, metal ions, and groups to help them undertake many other activities. MOF bimetal has a low over-potential. This is advantageous for ORR applications because of its wide-ranging metal valence, coordinated aromatic hydrocarbon sites, and atomic defects that provide static sites.

### 2.1. Advancement of MOFs

The perfect sacrificial templates for the thermal degradation of different NPCs, such as metal/metal oxide-decorated porosity, heteroatom-doped porous carbons, and porous carbons, in regulated conditions have recently been proven by MOFs consisting of metal ions and polyfunctional organic ligands [21]. When developing MOFs, it is necessary to ensure that all of the following conditions are met: (1) no agent that directs structure is present; (2) in light of the metal-ligand chemistry, it is reasonable to expect the specific structure formation, and it is possible to explain the existence of subtle synthetic variations by developing different morphology; (3) the reaction ought to be triggered by a reversible framework formation; and (4) the organic linker's composition must remain constant throughout the transesterification reaction [22]. The MOF template produced carbon-based materials, including a high-specific surface area, easily functionalized heteroatoms, and adaptable porosity over conventional hard- or soft-template methods [23]. Due to these advantages, much work on preparing various MOF-templated NPCs has been reported employing different MOF templates and temperatures, including additional precursors, pyrolysis, and further post-synthetic functionalization [24,25]. Organic ligands and metal ions formed by MOFs have large surface areas with adjustable porosities called porous composite materials. These materials are highly suitable for energy and environmental applications such as batteries. The MOFs are more applicable to anode materials in lithium-ion batteries because they afford porosity (channel), organic ligand, redox metal ion, and

electrolyte ion diffusion [26]. Additionally, metal ions and a network of metal clusters are present in porous, crystalline two- or three-dimensional structures. Hou et al. reported core–shell MOFs by control of thermal transformation, which showed open carbon cages such as the hydrangea superstructure in Figure 2. Direct pyrolysis may create an open-wall, carbon-caged structure, starting with a core–shell structure ( $\text{Zn-Co-MOFs}$ ). The open carbon-cage structure of the progenitors of core–shell MOFs changed into a hydrangea-like three-dimensional structure linked by carbon nanotubes when the guest ion (Fe) was introduced [27]. The core–shell ( $\text{Zn-Co-MOFs}$ ) pyrolysis produced Fe-Co alloy nanoparticles when Fe was introduced as a guest ion. Through hierarchically porous synergetic interactions between bimetallic functionalities (Co and Fe) and active catalytic sites in the metal nanoparticles, the superstructure exhibits good accessibility. These metallic bifunctional characteristics are ideal for ORRs and OERs in great energy applications (Zn-air battery).

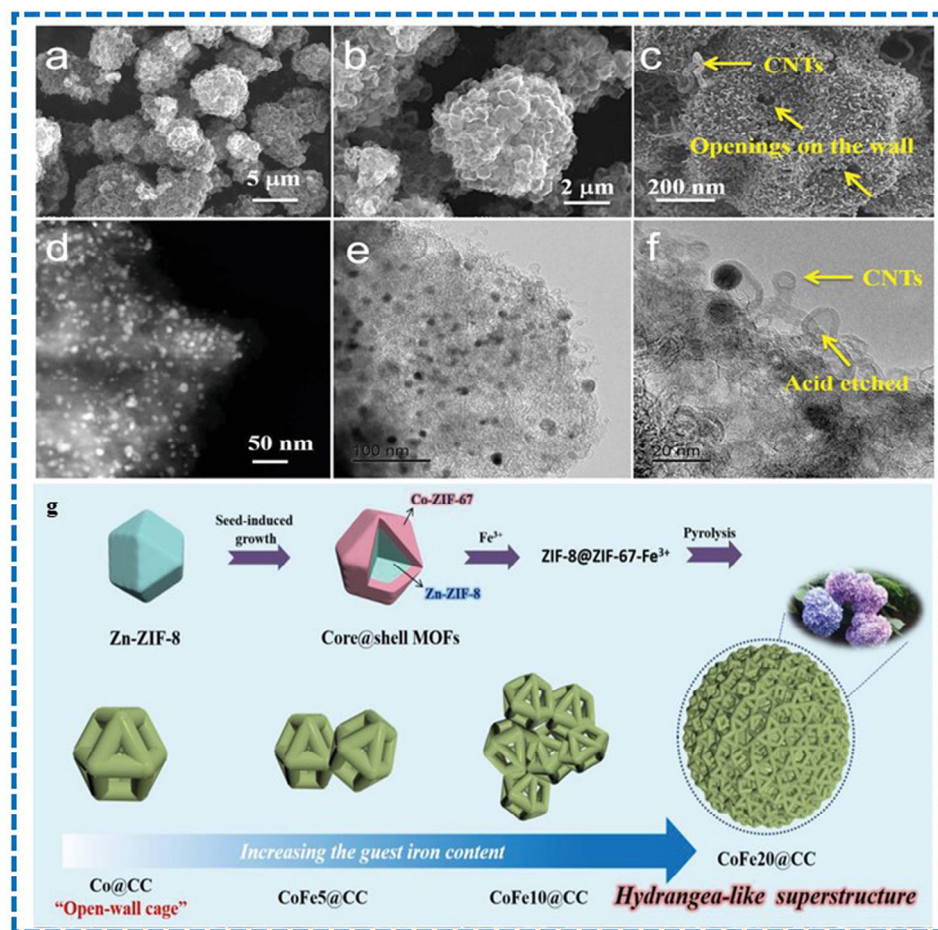


**Figure 2.** (a–c) Morphology of catalyst, (d) high-angle annular dark-field scanning transmission electron microscopy, and (e,f) transmission electron microscopy images of  $\text{CoFe}_{20}\text{@CC}$ . (g) Schematic illustration of the nature-inspired hydrangea-like superstructure from core–shell MOFs. Reproduced with permission from John Wiley and Sons [27].

## 2.2. MOF-Directed Tuning of Intrinsic and Extrinsic Frameworks

Extrinsic local forms in the MOF structure contrast with intrinsic local qualities, which include elemental compositions, dopants, and organic linkages with varying degrees of graphitization, size tuning, and porosity, among other things. Strong electronic transmission capacities might result from high graphitization [28]. Carbon-based MOF materials with a large surface area also expose more active sites and have quick reactant diffusion. As MOF can transfer the masses of electrolytes, oxygen, and ions, which are important properties for ORRs, size and porosity optimization are crucial. The surface-enrichment

effect, which strongly promotes electron transfer in the bifunctional metal-based chemical process, increases active area utilization in the MOF structure.

### 2.3. Influences of a High Graphitization Scale

The degree of graphitization in carbon-based materials is an essential material characteristic that boosts charge transfer efficiency. In the carbon-based MOF catalysts shown in Table 1, the degree of graphitization affects ORR performance. Bimetallic alloy (Fe-Co) has a carbon-cage structure that was developed according to Bu Guan et al. [29]. It exhibits outstanding electrochemical characteristics (ORR activity) in an alkaline media. By Huang et al., N and S were explored with Fe/Co nanoparticle doping to produce hierarchically porous carbon materials. It demonstrates how the interaction between various systems has improved [30]. In another study, Jing et al. analyzed the addition of an Ni catalyst into the CoFe nanoporous carbon. Adding Ni enhances the electrochemical reactions' ORR activities and long-term stability [31]. Al metal atoms were used to make a specific pyridinic N-doped porous carbon. According to research by Li et al., the pyridinic-N ligands enhance lower electron transfer at a high level of graphitization [32]. Using TiO<sub>2</sub>/Co metal ions, Jin et al. found a defect in nitrogen-doped carbon nanotubes (CNTs). While the electrochemical process occurs, the metal oxide (TiO<sub>2</sub>) resists severe corrosion and CO poisoning [33]. Guo et al. investigated the effects of porous N-doped CNT on the Fe/Co/Ni MOF system. Fe-NCNT exhibited more excellent ORR activity in this system than others [34]. By examination of the ORR performance comparison, it was determined that the incorporation of N into the metal site affects the electrochemical characteristics. The electronic conductivity of a material may be improved by using nanoparticles of metal. N doping and graphitization, on the other hand, support the idea of exposing more active MOF system regions. The high degree of graphitization contributes to a notable improvement in the intrinsic characteristics of MOF, particularly the surface area and porosity. According to a recent analysis, the degree of graphitization is a crucial component that directly influences ORR performance. Combining many major advantages into a single catalyst is the most effective strategy for maximizing the synergistic impact of these benefits.

**Table 1.** The effectiveness of MOF graphitization in ORR activity.

Sample	Hetero Atom	Metal Atom	Pyrolysis Temperature	ORR Applications	Ref.
Fe <sub>0.3</sub> Co <sub>0.7</sub> /NC cages	N	Fe, Co, and Zn	800 °C	0.98 V on set Potential	[29]
InFeCo-CNS900	N and S	Fe/Co	900 °C	59.5 mV dec <sup>-1</sup>	[30]
CoFeNi/N.C.	N	CoFeNi	800 °C	0.812 V	[31]
TiO <sub>2</sub> -NC-NCNTs	N	Ti/Co	900 °C	1.01 V	[33]
Pyridinic-N doped porous carbon (PNPC)	pyridinic-N	Al	1000 °C	0.890	[32]
ZnHKUST-1	N	Fe	1000 °C	0.997 V	[34]

### 2.4. Porous Structure Tuning

The use of electrochemical energy storage devices benefits more from a well-defined porosity. During the catalysis process and in the catalytic region, the porosity improves the mass transit of reactant access and product removal. Tuning the pores can make catalysis work better. One of the many ways to make MOFs could lead to creating an open structure. The self-assembly synthesis, pyrolysis, core–shell, and template processes are outlined in Figure 3.

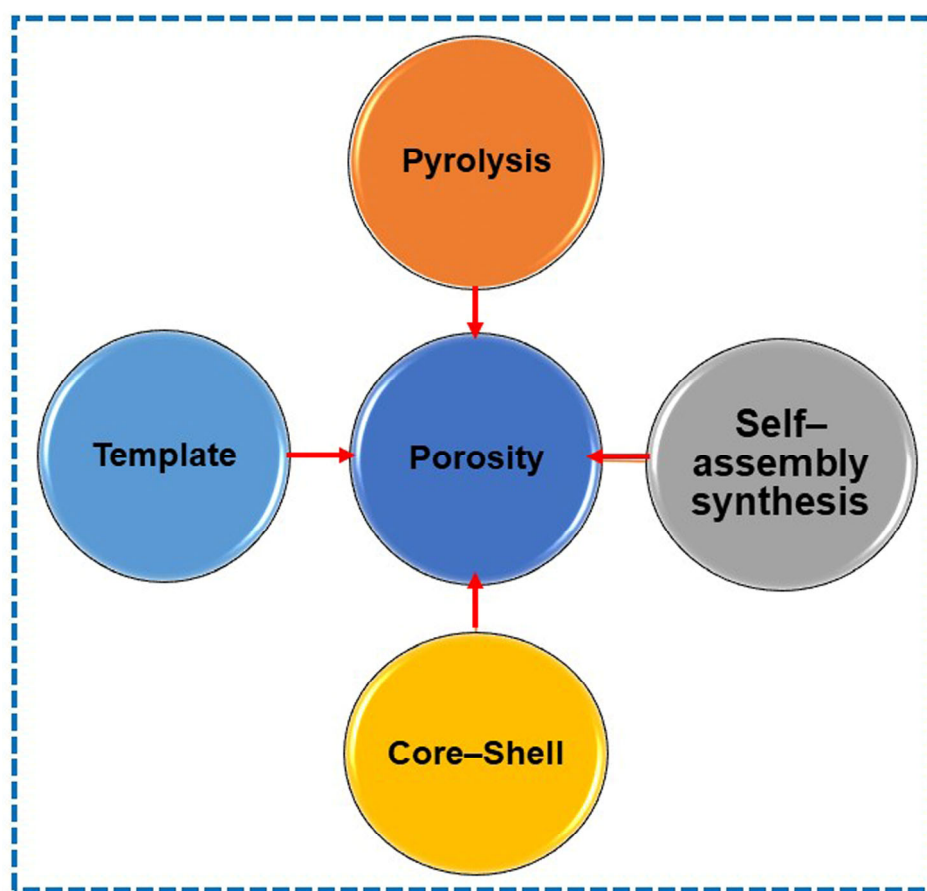


**Figure 3.** Schematic structure of porosity formation methods.

Rong et al. developed a two-dimensional porous catalyst (NP-CoSANC) by pyrolysis. During pyrolysis, adsorbed urea created a porous structure in the system, showing an effective surface area of  $634.8 \text{ m}^2 \text{ g}^{-1}$ . It offers an effective ORR performance ( $E_{1/2} = 0.86 \text{ V}$ ) in the alkaline medium (0.1M KOH) [35]. Chen et al. reported a three-dimensional interconnected porous structure developed by a melamine-assisted, template-free, co-calcined route. The structures (Fe-NMC) display the surface area with the quantity of melamine used. The rising concentration of melamine resulted in an increase in surface area from  $705.1 \text{ m}^2 \text{ g}^{-1}$  to  $844.9 \text{ m}^2 \text{ g}^{-1}$ . Fe-MNC-1 showed excellent ORR activity in acidic and alkaline media [36]. The electrocatalytic activities are boosted due to the design of the porous structure. Pyrolysis was used during the rational synthesis process to tune the porosity structure in MOF materials. As pores collapse when subjected to high temperatures, the pyrolysis process cannot link porous structures because the temperature is too high (over  $1100^\circ \text{C}$ ). Lu et al. recently studied a self-generating dual template to synthesize a porous MOF structure. This method obtained the surface area from 273 and  $531 \text{ m}^2 \text{ g}^{-1}$ , showing high electrochemical durability in ORR activity [37]. Nano-leaves were developed by Li and colleagues using a process called the sacrificial template approach. This approach formed a mesoporous structure, improving ORR activity [38]. Using the pyrolysis method, Guan et al. developed a pore using "MOF in MOF hybrid" (core-shell). Figure 4 displays the results of this sample preparation and the ORR activity. The  $\text{Fe}_{0.3}\text{Co}_{0.7}/\text{NC}$  porous cage structure performs excellent ORR activity. In addition to these methods, producing carbon with a wide surface area may also be accomplished by post-activation with potassium hydroxide [29].

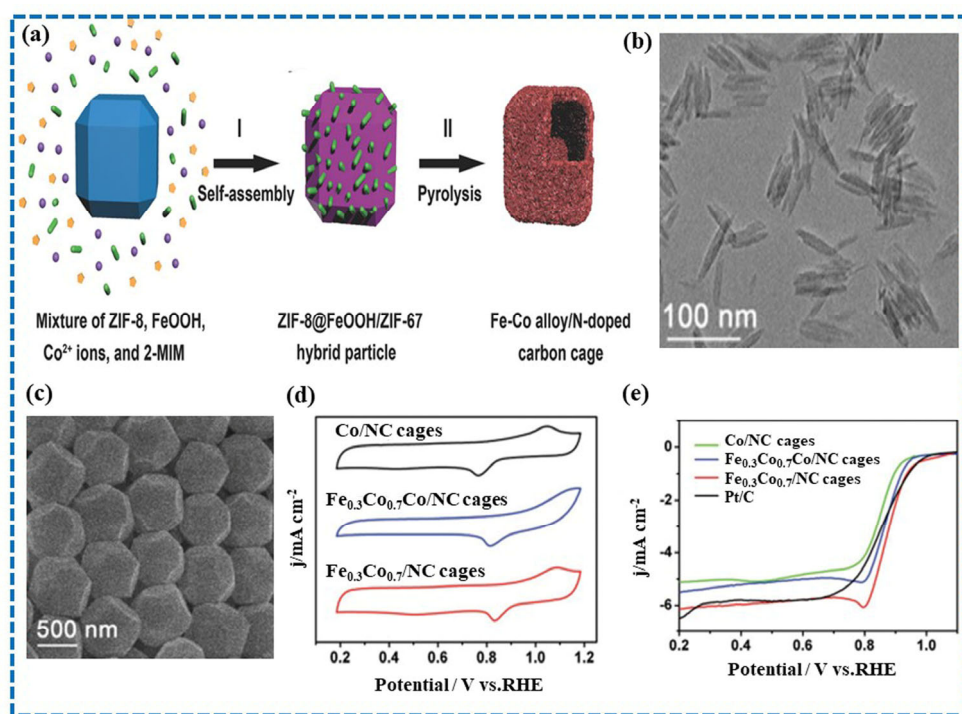


**Figure 4.** (a) Schematic illustration of the formation process of porous Fe-Co alloy/N doped carbon cages, (b) TEM images of ZIF-8 crystals (c) FE-SEM images of ZIF-8@FeOOH/ZIF-67 hybrid particles, (d) CV curves of in 0.1M KOH at 20 mVs<sup>-1</sup>, and (e) LSV plots in 0.1 M KOH solution at 10 mVs<sup>-1</sup>. Reproduced with permission from John Wiley and Sons [29].

## 2.5. The Influence of Size and Shape

The influence that the size of the catalyst has on the ORR is a substantial one, as is well acknowledged. It has been shown that the decrease in particle size of platinum nanoparticles used in platinum-based catalysts might increase the electrochemically active surface area of the catalyst [39]. Therefore, the size of the catalyst influences the activity of ORR performance when decreasing particle size. The pore size of porous MOFs may be modified, allowing for more or less control over the dimensions of the catalyst's active region. During the MOF synthesis process, the MOF size may be readily adjusted by making small adjustments to the synthetic conditions, pathways, and precursors. The catalyst's particle size may be readily adjusted using ZIF-67 as the precursor by varying the size of MOFs. Size-controlled MOFs were investigated by Xili et al. utilizing ZIF-67 precursors. ZIF-67 precursors may modify the particle size and shape of the Co-N-C active catalyst by switching between several solvents, including methanol, ethanol, and both combinations. By raising the concentration of methyl-imidazole, ZIF-67 size was managed. It demonstrates the long-term robustness of ORR in an alkaline medium with regulated particle size [40]. ORR activity that is dependent on particle size reductions was disclosed by Zhang et al. By varying the quantity of metal precursors and ligands, Fe is doped in the ZIF precursors. From 20 to 1000 nm might be the range for the crystal size. Fe-ZIF materials catalyst research relied on particle size, as shown in Figure 5a–d, which includes a schematic of the synthesis process and images of various particle sizes (1 μm, 200 nm, 50 nm, and 20 nm). With a continuously decreasing particle size, the E<sub>1/2</sub> value shifts in the positive direction. The Fe-ZIF catalyst performed ORR activity in the 0.5 M H<sub>2</sub>SO<sub>4</sub> and 0.1 M HClO<sub>4</sub> with functions of different particle sizes given in Figure 6a. Around 50 nm, particle size showed E<sub>1/2</sub> moved to the positive side, which indicates that the number of active areas increased with the reduction in particle size. The calculated H<sub>2</sub>O<sub>2</sub> production, potential cycle stability, and correlation between ORR activity and a given surface area (Sa) are all shown in Figure 6b–d. A smaller catalyst might provide a greater electrochemical active site, according to the findings of a correlation study between the BET-specific surface

area and MOF precursor crystal size. The catalyst with the highest ORR performance also reduced the particle size [41]. In light of this, the MOF-directed technique offers an easy way to produce efficient ORR catalysts while optimizing particle sizes.

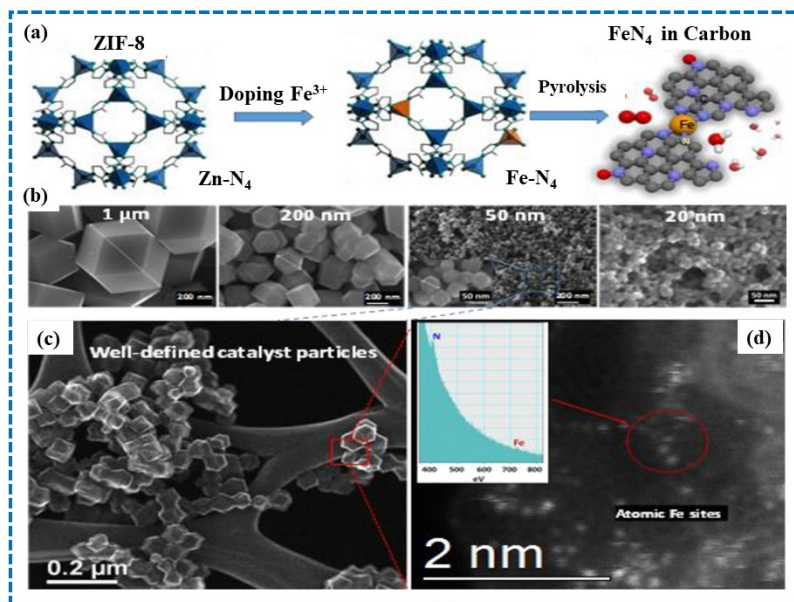


**Figure 5.** (a) The synthesis method of Fe-doped ZIF catalysts. (b) Particle size controlled from 20 to 1000 nm of Fe-doped ZIF catalysts. (c,d) 50 nm of Fe-doped ZIF catalyst's HAADF-STEM images and EELS analysis (the inset of (d)). Reproduced with permission from the American chemical society [41].

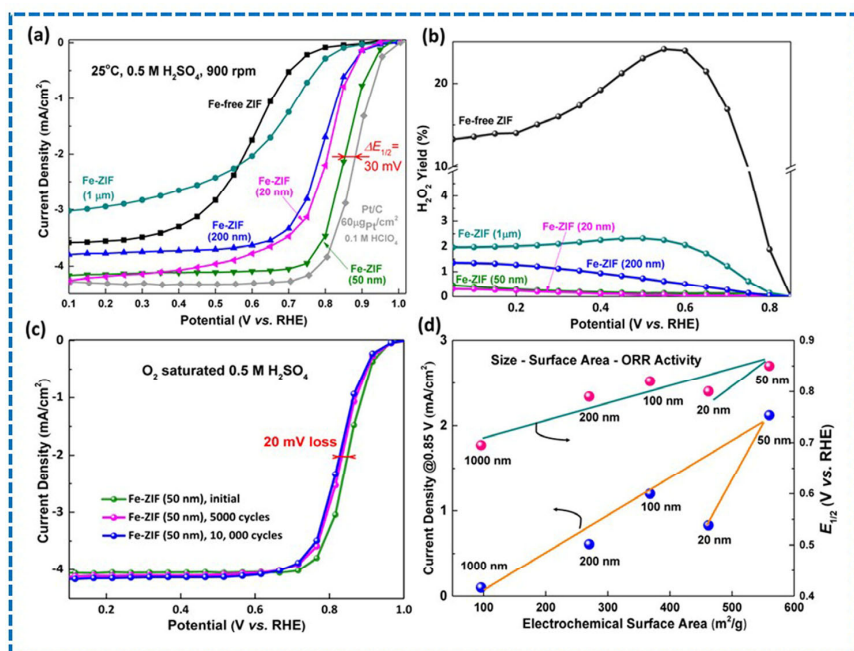
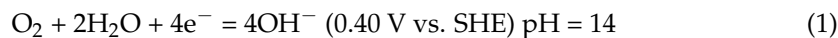


**Figure 6.** (a) ORR polarization curves of Fe-ZIF-derived catalysts in 0.5 M H<sub>2</sub>SO<sub>4</sub> and Pt/C catalysts (60 μgPt/cm<sup>2</sup>) in 0.1 M HClO<sub>4</sub> at 25 °C and 900 rpm. (b) Calculated H<sub>2</sub>O<sub>2</sub> from Fe-ZIF catalysts with particle size. (c) Cycling the potential (Stability in 0.6–1.0 V in O<sub>2</sub>-saturated 0.5 M H<sub>2</sub>SO<sub>4</sub>). (d) The relationship between ORR activity and clear size dependence. Reproduced with permission from the American chemical society [41].

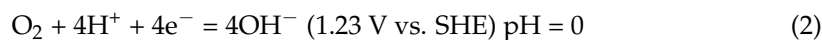
### 3. Oxygen Reduction Reaction (ORR) in MOFs

The multi-conjugated ORR reaction is a critical route in metal-air batteries and fuel cells. Traditionally, during the oxygen reduction reaction, catalysts undergo two different electrochemical processes. One of the efficient pathways is  $4e^-$  a pathway and the other is the sluggish  $2e^-$  pathway. Above this, the other track has additional thermodynamic kinetic potential in this ORR pathway [42,43]. The electrolyte medium and catalyst conditions are desirable for this complex reactional path. According to the theoretical approaches, the Yeager and Pauling model adsorption of oxygen molecules differs with the respective acid and alkaline mediums. Above  $4e^-$ , pathway water is consumed during the ORR without forming a peroxide intermediate. Initially, the  $4e^-$  pathway in alkaline and acid electrolyte solutions are as follows: Standard hydrogen electrode (V vs. SHE).

Alkaline medium:

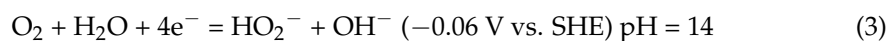


Acidic medium:



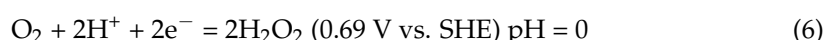
The  $2e^-$  ORR pathway generates intermediate  $H_2O_2$  formation and transforms into  $HO_2^-$ . This pathway disproportionate of  $H_2O_2$  leads to the formation of the intermediate  $OH^-$ .

Alkaline medium:



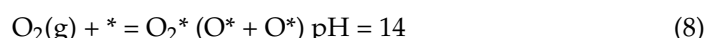
The direct double-step, two-electron pathway includes the following steps during the ORR process.

Acid medium:



In the electrocatalytic matrix developments, combining the  $HOO^*$  and  $O_2$  absorption and desorption pathways leads to exploring the elementary steps in the ORR reaction. The following O–O bond cleavage determining steps is one of the extensive phenomena in this ORR mechanism pathway. In alkaline medium, intermediate hydronium species act as a Lewis basic (donate the proton) following elementary steps in the ORR process in the alkaline medium.

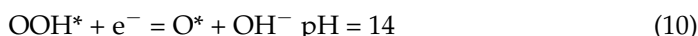
- Associative and dissociative appears on the surface of the catalysts:



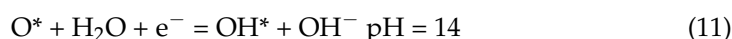
- Electron transfer from anode region to associative  $O_2$ :



- Intermediate O=O dissociation:

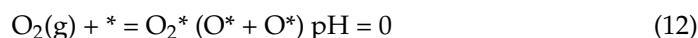


- Generation of OH<sup>-</sup> from catalysts surface to solution:

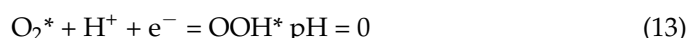


Primary elementary steps in acid medium with respect to O<sup>\*</sup>, OH<sup>\*</sup>, and HOO<sup>\*</sup> adsorbed intermediates.

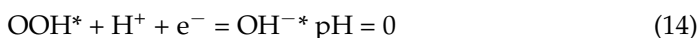
- Associative O<sub>2</sub> appears on the surface of the catalysts.



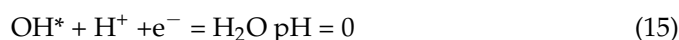
- Electron transfer from anode to associative O<sub>2</sub>.



- Intermediate dissociation.



- Generation of the H<sub>2</sub>O byproduct from the ORR pathway.



In the ORR pathway process, the 4e<sup>-</sup> transfers higher voltage than the 2e<sup>-</sup> pathway. MOF-derived single-metallic, bi-metallic, and multi-metallic metal-nitrogen matrix (M-N<sub>x</sub>) moieties always prefer to lead the four-electron reduction pathway for producing the water byproduct from oxygen. Generally, the macrocyclic transition metallic nitrogen carbon complexes (TM-N-C) are not more stable in electrolytes, especially in alkaline electrolytes medium. MOF-derived TM-NC catalysts have a high surface area due to the high thermal pyrolysis treatment. The above ORR mechanism was well attributed to the MOF-derived TM-NC catalysts [44]. The metal cation and organic ligands coordination sites increase the graphitization in the catalyst's surface. Pyridine, pyrrolidine, and oxidized metal sites are one of the facilitated active sites in the MOF-derived metal catalysts. π-π stacking between the cyclic ligands and metal cation sites increases the charge transfer phenomena during the dissociation and association intermediate stages [45]. The MOF-derived M-N<sub>4</sub> sites increase the active region collision between the electrode and electrolytes [46]. Well-defined structural architecture and single-atom distributions majorly act as a rate-determining step in the oxygen reduction reaction in alkaline and acid media.

#### 4. MOF Derivatives

The design of MOFs enables uniform distribution of the active sites in the produced catalysts. Due to its various uses, an MOF transforms into an effective substance with a substantial porous area that accepts foreign materials. Metals, porous carbons, metal oxides, metal phosphides, heteroatomic carbons, and other novel materials have been synthesized using MOFs as precursors [47–49]. MOFs can also be used as host materials or sacrificial agents to produce metals such as nitrogen and carbon. For instance, it may provide a porous, high-surface-area structure and boost the effectiveness of the catalytic function in ORR systems. MOF particle size, metal base, and porous structure may favorably influence the catalyst's capacity to attain high performance. The synergistic interaction between ligands and metal atoms in the MOF structure makes it appropriate for electrical structures, boosts the activity of ORR catalysts, and enhances mass transfer. Similarly, a three-dimensional MOF structure provides an active site to attack elements. In situ growth of graphene or CNTs is used to make MOF assemblies because these materials act as carriers [50]. Metal

ions and organic ligands provide a versatile framework for driving porous and crystalline MOF structures. By varying the structural characteristics of these special elements, MOF derivatives may have smoother structures. Numerous derivatives of MOFs are available, each with distinct pore-size characteristics, active metal sites, and surface area. Here, we go through various MOF derivatives for ORR applications, including metal phosphide in MOFs, metal oxide in MOFs, and SAC in MOF porous carbon composites.

#### 4.1. Single-Atom Catalyst (SAC) in MOFs for ORR

In 1995, Thomas et al. reported on SAC features for catalytic applications. The SAC has unique properties (physical and chemical) by geometry size reduction. In the SAC, maximum active site utilization and exclusive electronic properties are achieved by the quantum size effect, which applies to a vast range of catalytic reactions. However, SACs may not be stable during synthesis and could be aggregated by high-energy particles. Therefore, the SAC needs a substrate to explore its unique properties. In this regard, MOFs provide a strong foundation for customizing the porous architecture, large surface area, and SAC construction [51]. Figure 7 illustrates the comparative analysis of SACs with conventional porous materials.

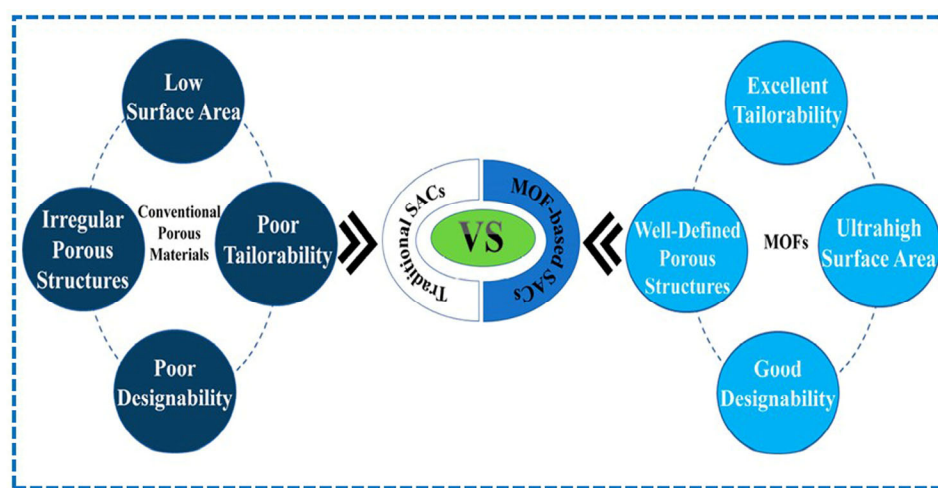


**Figure 7.** Comparative analysis of MOF-supported SACs with traditional SACs. Reproduced with permission from the American chemical society [51].

MOF-based SACs have remarkable properties, such as high surface area, good designability, porous structures, and excellent tailoring structures compared to traditional SACs. The MOF-based SAC was developed in two steps: MOF-stabilized SAC and MOF-derived SAC. The MOF-stabilized SAC is a limited method under mild conditions. This method makes property achievement challenging due to aggregation in high metal ion loading. However, MOF-derived SACs show excellent durability compared with MOF-stabilized SACs. They can be prepared by the pyrolysis method via mixed metal, spatial confinement, and mixed-ligand approaches. During pyrolysis, ligand-derived N atom bonds with metal via coordination interaction, which resists the agglomeration of metal atoms in the porous carbon network. Therefore, an MOF is a good platform to develop SACs for ORR catalysts, with plenty of tunable properties to accommodate SACs. Zhou et al. recently reported on Co-composed 3D star MOFs for ORR applications. The metal atom (Co) doped in ZIF-8 and ZIF-L precursors showed Co-N<sub>3</sub>C SACs by pyrolysis. The developed SACs (CoSA-N-C) exhibited high ORR activity with E<sub>1/2</sub> (0.891 V) in 0.1 M KOH [52]. The novel approach decreases the free energy barrier in ORR reactions. Ding et al. studied Fe doped in the ZIF precursors, which forms an Fe-N<sub>4</sub> matrix with various particle size distributions. At 50 nm particle size, it shows excellent ORR activity with E<sub>1/2</sub> of 0.85 V in 0.5 M H<sub>2</sub>SO<sub>4</sub>. At high temperatures, the synergistic effect between graphitic N

and F-N4 enhances ORR activity [53]. Xie et al. published Fe atom-doped MOF-5 substrates for ORR activity. The MOF-5 substrate shows a high surface area ( $>3000\text{ m}^2\text{g}^{-1}$ ), which supports accommodating the  $\text{FeN}_x$  active area. In the system (Fe SAC-MOF-5), Fe ions are doped by the ligand-mediated method, and during this, high Fe ions are loaded in the MOF-5 support due to the large surface area. Fe SAC-MOF-5 exhibited an  $E_{1/2}$  of 0.83 V in an acid medium (0.5 M  $\text{H}_2\text{SO}_4$ ) in the ORR activity [54]. The high surface area (ultra) of MOF-based porous carbon performs excellent ORR activity in PEMFCs. At the same time, pyrrolic-N-rich carbon support increases the number of metal sites by the electronegative difference between pyrrolic-N and metal atoms (Fe). Li et al. studied a novel approach for ORR catalysts, such as Fe-N<sub>4</sub> dispersed on the MOF-derived graphene mesh. Nitrogen-doped graphene (NGM) mesh was prepared using the thermal exfoliation technique from ZIF. The control of the exfoliation process modifies the shape and size of the pores. Fe atoms are dispersed by the pyrolysis method using ideal Fe precursors, which resulted in SA-Fe-NGM catalyst. The catalyst (SA-Fe-NGM) studied ORR activity in 0.5 M  $\text{H}_2\text{SO}_4$  ( $E_{1/2} = 0.83\text{ V}$ ) and delivered 634 mW  $\text{cm}^{-2}$  power density in the fuel cell test [55]. The catalyst preparation methodology and ORR activity are given in Figure 8. Wang et al. studied Fe metal doped in the heteroatom (S)-doped MOF matrix. It was successfully prepared using a low temperature freezing pyrolysis method. The sulfur atom prevents metal ions from clumping together in the MOF substrate [56]. Overall, high surface area and large porosity MOFs are more suitable for SAC doping to enhance ORR activity. However, to attain selective pore size and high surface area, the selection of precursors and preparation temperature is challenging to develop effective SAC doping in the MOF matrix.

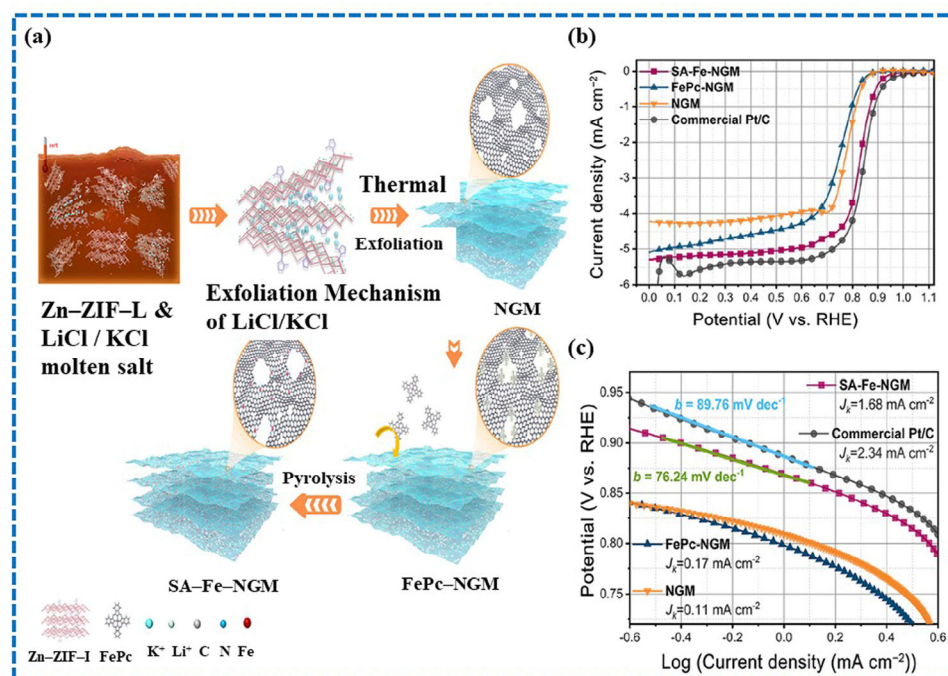


**Figure 8.** (a) Preparation of SA-Fe-NGM catalyst. (b) LSV polarization plots were recorded at 1600 rpm with a scan rate of 5 mV s<sup>-1</sup>. (c) Tafel plot of corresponding LSV curves. Reproduced with permission from the American chemical society [55].

#### 4.2. MOF–Carbon Composite

Carbon-based MOF composites have gained attention in ORR activity due to the increase in the extrinsic properties of the MOF matrix. MOF–carbon composites facilitate high conductivity when the pyrolysis temperature, degree of graphitization, and precursors are adjusted. Carbon’s terminal groups induce dipole polarization via electronegativity, which improves the dispersion of SACs, metal oxides, nanoparticles, and other compounds in the MOF–carbon composite. The study and exploration of MOF–carbon composites

have recently seen significant advancement in the ORR catalyst. According to Anwar et al., carbon-based electrocatalysts derived from mass transport in MOFs is extremely effective in electrochemical processes due to their pore structure [57]. In addition, active catalyst sites may be developed with MOF–carbon, which has a large surface area and pore size. The metal–organic gaseous technique produced Fe-doped, MOF-derived carbon [58]. Its catalytic activity and stability are outstanding in both acidic and alkaline environments. Wang et al. reported on MOF-based carbon nanotubes (Fe/N–CNT) through pyrolysis using Fe-ZIF-8 and g-C<sub>3</sub>N<sub>4</sub> precursors. The ORR activity performed well because of the high conductivity, large pore volume, and specific surface area of carbon nanotubes. The Fe/N–CNT catalyst showed a half-wave potential of 0.892 V and 0.79V in 0.1 M KOH and 0.1 M HClO<sub>4</sub>, respectively. It also improves stability and methanol resistance compared to commercial Pt/C catalysts [59]. A crucial interaction between MOF–carbon composites and other components and structures helps to enhance their new chemical and physical capabilities. MOF–carbon composites have the potential to result in the development of new synthetic processes that are more effective and efficient, have greater activity, are durable, and have high electrocatalytic stability. It improves the stability and effectiveness in the application reaction (ORR). According to Yang and colleagues, metallic and porous carbon hybrids that are generated from MOFs have the potential to be catalysts. They are extremely resilient to heteroatom doping. The particular active region of MOFs is exposed in large amounts to hasten the mass transfer process. ZIF precursors have been confirmed as potential candidates for synthesizing functional carbon materials using the carbonization method in an inert atmosphere [47]. MOF-5-derived carbon reportedly has excellent physiochemical characteristics for the electrochemical activities of fuel cell applications, as stated by Khan et al. [60]. A nitrogen-doped porous carbon electrocatalyst was developed using an MOF-derived precursor. These types of catalysts show hierarchical porosity, heterostructure conductivity, long-term stability, and good ORR activity (excellent onset and E<sub>1/2</sub>) in an alkaline medium. The MOF-derived carbon composites have several advantages over activated carbon, graphene, and carbon nanotubes. The MOF-derived carbon has the feasibility of controlled pore size and shape, heteroatom doping via organic ligands, and high surface area. However, the manufacturing cost is relatively higher than traditional carbons.

#### 4.3. Metal Oxides Derived from MOFs

Generally, transition metal oxides are applied as a catalyst. However, they show poor conductivity and could not be used in fuel cell applications. Therefore, metal oxide-derived MOFs improve their catalytic properties because metal oxide covers an additional layer, similar to carbon from MOF precursors. Metal oxide/nanocarbon composite catalysts derived from MOFs have enhanced the interactions between the metal oxide and the nanocarbon matrix. This can significantly increase the catalyst's activity. Gamal et al. reported on spinal oxide-supported TiO<sub>2</sub>/carbon from MOF (MIL-125) for electrocatalyst applications. Nanocrystalline NiCo<sub>2</sub>O<sub>4</sub> provides a more redox-active site for oxygen absorption and activation. This spinal-type structure resulted in high electrical conductivity. The NiCo<sub>2</sub>O<sub>4</sub>/Es-TiO<sub>2</sub>/NC catalyst showed similar ORR activity to the Pt/C in an alkaline medium, and it exhibited methanol resistance and higher stability than the Pt/C catalyst [61]. Kuang et al. studied Co<sub>3</sub>O<sub>4</sub> nanoparticles incorporated into MOF nanofibers on C- and N-supported Ni foam by self-assembly [62]. Co(II)-MOF fibers were prepared by electrolysis at room temperature. Carbon and nitrogen arrays on Co(II)-MOF (Co<sub>3</sub>O<sub>4</sub>–C–N N.S.A./NiF) were prepared by pyrolysis at 300 °C. The sp<sup>2</sup> carbon and nitrogen array boost the more active sites and mass transport. This catalyst exhibited high turnover frequency (0.958 s<sup>-1</sup>), low resistance, and long durability in the overpotential of 370 mV. Niu et al. researched an electrocatalyst made of Fe<sub>2</sub>O<sub>3</sub>-MOF. When considering the catalytic activity, multivalent iron ions are preferred to other transition metal oxides [63]. The researcher prepared Fe<sub>2</sub>O<sub>3</sub> from MOF precursors to obtain different types of morphologies, such as concave octahedral, rod-like, spindle-like, and octahedron-like Fe-MOFs, as given in

Figure 9. The concave octahedral  $\text{Fe}_2\text{O}_3$  illustrated a large surface area, active lattice planes, and hierarchical porosity to a greater extent than other morphologies. Due to this, they have the perfect characteristics for functioning as an ORR catalyst. Xu et al. studied a Co–CoO– $\text{Co}_3\text{O}_4$ –N/C catalyst from MOF precursors by thermal treatment, as a prepared catalyst has a higher current-limiting density ( $4.9 \text{ mA cm}^{-2}$ ) and onset potential ( $0.136 \text{ V vs Ag/AgCl}$ ) [64]. It showed good methanol tolerance and 80% stability in ORR performance. The Co and CoO are uniformly dispersed in Co-Nx, enhancing their synergistic effect. That effect improves mass transport and catalytic reactions. Cobalt oxide has been widely derived from MOF precursors, more so than from Fe and Ni oxides [65]. MOF-derived metal oxide provides excellent electrocatalytic activity when compared to conventional metal oxide. The MOF platform has unique features to develop active metal oxide-based electrocatalysts. However, selecting MOF precursors, temperature, and synthesis methods are crucial to obtaining a highly porous metal oxide-derived MOF for ORR catalysts.

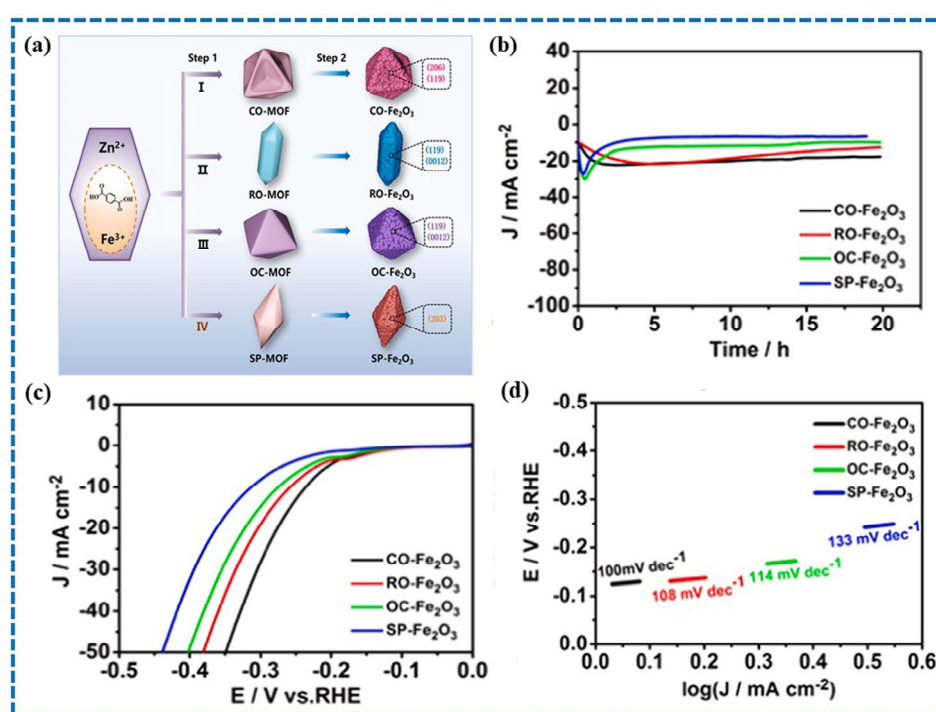


**Figure 9.** (a) Schematic illustration of the synthetic process of  $\text{Fe}_2\text{O}_3$  with different morphologies and structures via solvothermal synthesis under other ions- and solvent-controlled systems and pyrolysis in Ar. (b) Cyclic voltammetry (CV) curves of CO, RO, OC, and SP- $\text{Fe}_2\text{O}_3$  in nitrogen- or oxygen-saturated 0.1 M KOH solution. (c) Linear sweep voltammetry (LSV) plots of CO, RO, OC, and SP- $\text{Fe}_2\text{O}_3$  at 1600 rpm. (d) Tafel slopes of CO, RO, OC, and SP- $\text{Fe}_2\text{O}_3$ . Reproduced with permission from John Wiley and Sons [63].

#### 4.4. Metal Phosphide Derived from MOFs

An MOF is an ideal platform to synthesize the varied composition of the element under a variety of synthetic settings, and this is because an MOF is a metal–organic framework. MOF precursors may also produce transition metal phosphides, commonly known as TMSs, which can be used in electrocatalytic processes. As phosphorus has a matic structure, it is difficult for phosphate molecules to fit into the pores of the MOF. For this reason, researchers are concentrating on various morphologies and sizes of TMSs to develop more effective applications. Sun et al. reported  $\text{Ni}_2\text{P}$  on Co- and N-doped porous MOFs ( $\text{Ni}_2\text{P}/\text{CoN-PCP}$ ). CoN-PCP prevents agglomeration of  $\text{Ni}_2\text{P}$ , and the CoN-PCP affords a highly exposed active area and high mass transfer for excellent ORR activity [66].  $\text{Ni}_2\text{P}/\text{CoN-PCP}$  showed  $E_{1/2}$  of 0.871 V for ORR activity at an alkaline medium in Figure 10.

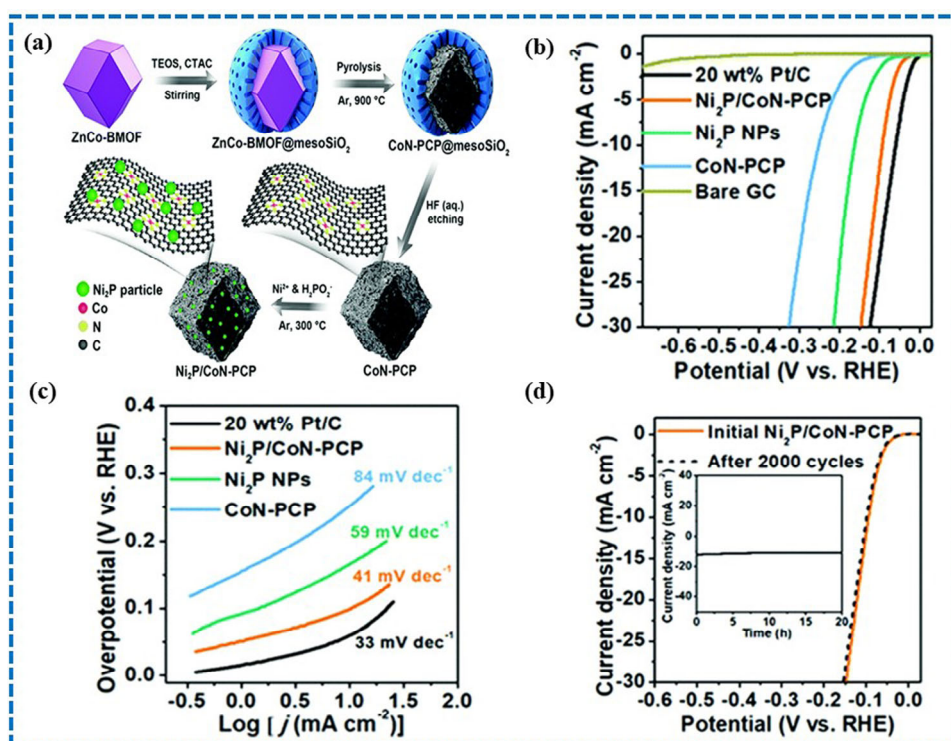


**Figure 10.** (a) Schematic design for preparing Ni<sub>2</sub>P/CoN-PCP, (b) ORR LSV curves for the studied catalysts. (c) ORR LSV images of Ni<sub>2</sub>P/CoN-PCP at various rotating rates, inset: K-L plots of Ni<sub>2</sub>P/CoN-PCP and Pt/C at different potentials. (d) ORR LSV plots before and after 2000 cycles. Reproduced with permission from the Royal Society of Chemistry [66].

P/Ni/Co/NC electrocatalysts were prepared using ZIF-67 precursors by Li et al. Ni/P doped by the pyrolysis of Co-NC at 800 °C shows the dodecahedral and hollow structure morphology. This electrocatalyst exhibited a Tafel slope of 64 mV/dec, a smaller value than Ni/Co/NC. Therefore, metal phosphides boost electrocatalytic reactions [67]. Likewise, Li et al. studied Co/CoP applied in an N-doped MOF structure. The ZIF-67 precursors were subjected to thermal pyrolysis at a temperature of 700 °C, which resulted in the formation of the catalyst Co-NC-CoP-NC [68]. In the ORR activity, the kinetic current density (0.7 V) and onset potential are similar to the Co compound from ZIF-67 precursors. Tang et al. produced Co–Co<sub>2</sub>P–NC–P catalysts for electrocatalytic applications (ORR). The researcher prepared this catalyst by doping high N and P ligands using an in-situ method. The phosphorus contains ligands synthesized from 2-methylimidazole and diammonium hydrogen phosphate (NH<sub>4</sub>)<sub>2</sub>HPO<sub>4</sub>. It shows the porous structure loosely, improving durability and stability during electrochemical analysis [69]. Only a few researchers have reported on the nanostructured metal phosphides derived from MOF precursors for electrocatalytic activity. The variety of metal phosphides from MOFs is required to maximize the chance of the electrocatalyst cooperating synergistically.

## 5. Conclusions and Perspectives

MOFs have broadened opportunities in the field of electrocatalysts for energy applications. MOF precursors are a good platform for turning the intrinsic and extrinsic properties of electrocatalysts. These properties mainly depend on selecting precursors, temperature, and preparation methods. We can harvest unique features from tunable morphology, pore size, and specific surface area from the MOF matrix. Conventional MOFs have limited the properties of electrical conductivities, which have improved by manipulating MOF-derived composites such as SAC-MOF, carbon-based MOF composites, metal-oxide MOFs, and metal-phosphide MOFs. Among these catalyst types, SAC-MOF has achieved good performance in ORR applications. Recently, carbon nanotube-based porous matrix-supported

electrocatalysts have been successfully discovered for ORR applications. From this perspective, the metal phosphide MOF needs to be explored more for ORR activity in fuel cell applications. For the innovative design and unique feature of MOF electrocatalysts, we must add a computational tool for excellent performance. Focusing on preparing effective MOF precursors will be derived from high-end electrocatalysts for ORR application in fuel cells. This review may help to design novel MOF-based electrocatalysts for ORR application in green energy generation.

**Author Contributions:** Conceptualization, K.D. and M.P.; methodology, K.D. and G.S.; validation, K.D., T.S. and T.H.O.; formal analysis, K.D. and N.M.; investigation, K.D.; resources, K.D. and N.M.; data curation, K.D.; writing—original draft preparation, K.D., M.P., G.S., N.M., S. and T.S.; writing—review and editing, K.D. and T.H.O.; visualization, K.D., T.S. and T.H.O.; supervision, T.H.O.; project administration, K.D., T.S. and T.H.O.; funding acquisition, T.H.O. All authors have read and agreed to the published version of the manuscript.

**Funding:** This research was supported by Yeungnam University research grants in 2023. The authors acknowledge the National Research Foundation of Korea grant sponsored by the Korean government (MIST) (No. 2022R1A2C1004283) and the Research Center for Natural Products and Medical Materials (RCNM) at Yeungnam University.

**Data Availability Statement:** Not applicable.

**Conflicts of Interest:** The authors declare no conflict of interest.

## References

- Baz, K.; Cheng, J.; Xu, D.; Abbas, K.; Ali, I.; Ali, H.; Fang, C. Asymmetric impact of fossil fuel and renewable energy consumption on economic growth: A nonlinear technique. *Energy* **2021**, *226*, 120357. [[CrossRef](#)]
- Hunt, J.D.; Nascimento, A.; Nascimento, N.; Vieira, L.W.; Romero, O.J. Possible pathways for oil and gas companies in a sustainable future: From the perspective of a hydrogen economy. *Renew. Sustain. Energy Rev.* **2022**, *160*, 112291. [[CrossRef](#)]
- Kataria, A.; Khan, T.I. Necessity of Paradigm Shift from Non-renewable Sources to Renewable Sources for Energy Demand. In *Urban Growth and Environmental Issues in India*; Kateja, A., Jain, R., Eds.; Springer: Singapore, 2021; pp. 337–352. [[CrossRef](#)]
- Sadhasivam, T.; Dhanabalan, K.; Roh, S.-H.; Kim, T.-H.; Park, K.-W.; Jung, S.; Kurkuri, M.D.; Jung, H.-Y. A comprehensive review on unitized regenerative fuel cells: Crucial challenges and developments. *Int. J. Hydrol. Energy* **2017**, *42*, 4415–4433. [[CrossRef](#)]
- Dhanabalan, K.; Sadhasivam, T.; Park, J.H.; Jung, H.Y.; Kim, B.S.; Roh, S.H. Advances in Metal–Organic Ligand Systems for Polymer Electrolyte Membranes: A Review. *Fuel Cells* **2017**, *17*, 278–287. [[CrossRef](#)]
- Etesami, M.; Mehdipour-Ataei, S.; Somwangthanaroj, A.; Kheawhom, S. Recent progress of electrocatalysts for hydrogen proton exchange membrane fuel cells. *Int. J. Hydrol. Energy* **2022**, *47*, 41956–41973. [[CrossRef](#)]
- Wu, D.; Shen, X.; Pan, Y.; Yao, L.; Peng, Z. Platinum Alloy Catalysts for Oxygen Reduction Reaction: Advances, Challenges and Perspectives. *ChemNanoMat* **2020**, *6*, 32–41. [[CrossRef](#)]
- Abd Aziz, A.J.; Baharuddin, N.A.; Somalu, M.R.; Muchtar, A. Review of composite cathodes for intermediate-temperature solid oxide fuel cell applications. *Ceram. Int.* **2020**, *46*, 23314–23325. [[CrossRef](#)]
- Alipour Moghadam Esfahani, R.; Kong, F.; Black-Araujo, K.; Easton, L.J.; Ebralidze, I.I.; Easton, E.B. A doped metal oxide PGM-free electrocatalyst for the oxygen reduction reaction. *Electrochim. Acta* **2023**, *438*, 141564. [[CrossRef](#)]
- Osmieri, L. Transition metal–nitrogen–carbon (M–N–C) catalysts for oxygen reduction reaction. Insights on synthesis and performance in polymer electrolyte fuel cells. *ChemEngineering* **2019**, *3*, 16. [[CrossRef](#)]
- Wang, R.; Lou, M.; Zhang, J.; Sun, Z.; Li, Z.; Wen, P. Zif-8@zif-67-derived co embedded into nitrogen-doped carbon nanotube hollow porous carbon supported pt as an efficient electrocatalyst for methanol oxidation. *Nanomaterials* **2021**, *11*, 2491. [[CrossRef](#)]
- Zhang, B.; Chen, R.; Yang, Z.; Chen, Y.; Zhou, L.; Yuan, Y. Rapeseed meal-based autochthonous N and S-doped non-metallic porous carbon electrode material for oxygen reduction reaction catalysis. *Int. J. Hydrol. Energy* **2021**, *46*, 508–517. [[CrossRef](#)]
- Chen, K.; Shi, L.; Zhang, Y.; Liu, Z. Scalable chemical-vapour-deposition growth of three-dimensional graphene materials towards energy-related applications. *Chem. Soc. Rev.* **2018**, *47*, 3018–3036. [[CrossRef](#)]
- Khan, J.; Liu, H.; Xiao, J.; Zhu, Y.; Hayat, A.; Ullah, H.; Ahmed, G.; Zhang, H.; Sun, Y.; Han, L. Synthesis of heteroatom incorporated porous carbon encapsulated Fe-doped Co<sub>9</sub>S<sub>8</sub> as an efficient bifunctional electrocatalyst for overall water splitting. *J. Phys. Chem. Solids* **2023**, *175*, 111220. [[CrossRef](#)]
- Wang, W.; Xu, X.; Zhou, W.; Shao, Z. Recent Progress in Metal-Organic Frameworks for Applications in Electrocatalytic and Photocatalytic Water Splitting. *Adv. Sci.* **2017**, *4*, 1600371. [[CrossRef](#)]
- Zhou, J.; Zeng, C.; Ou, H.; Yang, Q.; Xie, Q.; Zeb, A.; Lin, X.; Ali, Z.; Hu, L. Metal-organic framework-based materials for full cell systems: A review. *J. Mater. Chem. C Mater.* **2021**, *9*, 11030–11058. [[CrossRef](#)]
- Dang, S.; Zhu, Q.L.; Xu, Q. Nanomaterials derived from metal-organic frameworks. *Nat. Rev. Mater.* **2017**, *3*, 17075. [[CrossRef](#)]

18. Hu, Y.; Liu, J.; Lee, C.; Li, M.; Han, B.; Wu, T.; Pan, H.; Geng, D.; Yan, Q. Integration of Metal–Organic Frameworks and Metals: Synergy for Electrocatalysis. *Small* **2023**, *23*, 2300916. [[CrossRef](#)]
19. Li, Y.; Xu, Y.; Yang, W.; Shen, W.; Xue, H.; Pang, H. MOF-Derived Metal Oxide Composites for Advanced Electrochemical Energy Storage. *Small* **2018**, *14*, 1704435. [[CrossRef](#)]
20. Jiao, L.; Jiang, H.L. Metal-Organic-Framework-Based Single-Atom Catalysts for Energy Applications. *Chem* **2019**, *5*, 786–804. [[CrossRef](#)]
21. Shen, K.; Chen, X.; Chen, J.; Li, Y. Development of MOF-Derived Carbon-Based Nanomaterials for Efficient Catalysis. *ACS Catal.* **2016**, *6*, 5887–5903. [[CrossRef](#)]
22. Zhang, Y.; Feng, X.; Yuan, S.; Zhou, J.; Wang, B. Challenges and recent advances in MOF-polymer composite membranes for gas separation. *Inorg. Chem. Front.* **2016**, *3*, 896–909. [[CrossRef](#)]
23. Li, K.; Yang, J.; Gu, J. Hierarchically Porous MOFs Synthesized by Soft-Template Strategies. *Acc. Chem. Res.* **2022**, *55*, 2235–2247. [[CrossRef](#)] [[PubMed](#)]
24. Wang, S.; Liu, L.; Wang, S.M.; Han, Z. MOF-templated nitrogen-doped porous carbon materials as efficient electrocatalysts for oxygen reduction reactions. *Inorg. Chem. Front.* **2017**, *4*, 1231–1237. [[CrossRef](#)]
25. Nath, K.; Bhunia, K.; Pradhan, D.; Biradha, K. MOF-templated cobalt nanoparticles embedded in nitrogen-doped porous carbon: A bifunctional electrocatalyst for overall water splitting. *Nanoscale Adv.* **2019**, *1*, 2293–2302. [[CrossRef](#)] [[PubMed](#)]
26. Yin, C.; Pan, Y.; Pan, C.; Xu, L. Metal–organic framework as anode materials for lithium-ion batteries with high capacity and rate performance. *ACS Appl. Energy Mater.* **2020**, *3*, 10776–10786. [[CrossRef](#)]
27. Hou, C.C.; Zou, L.; Xu, Q. A Hydrangea-Like Superstructure of Open Carbon Cages with Hierarchical Porosity and Highly Active Metal Sites. *Adv. Mater.* **2019**, *31*, 1904689. [[CrossRef](#)]
28. Fuchs, A.; Mannhardt, P.; Hirschle, P.; Wang, H.; Zaytseva, I.; Ji, Z.; Yaghi, O.; Wuttke, S.; Ploetz, E. Single Crystals Heterogeneity Impacts the Intrinsic and Extrinsic Properties of Metal–Organic Frameworks. *Adv. Mater.* **2022**, *34*, 2104530. [[CrossRef](#)]
29. Guan, B.Y.; Lu, Y.; Wang, Y.; Wu, M.; Lou, X.W.D. Porous Iron–Cobalt Alloy/Nitrogen-Doped Carbon Cages Synthesized via Pyrolysis of Complex Metal–Organic Framework Hybrids for Oxygen Reduction. *Adv. Funct. Mater.* **2018**, *28*, 1706738. [[CrossRef](#)]
30. Huang, Q.; Guo, Y.; Wang, X.; Chai, L.; Ding, J.; Zhong, L.; Li, T.-T.; Hu, Y.; Qian, J.; Huang, S. In-MOF-derived ultrathin heteroatom-doped carbon nanosheets for improving oxygen reduction. *Nanoscale* **2020**, *12*, 10019–10025. [[CrossRef](#)]
31. Jing, Y.; Cheng, Y.; Wang, L.; Liu, Y.; Yu, B.; Yang, C. MOF-derived Co, Fe, and Ni co-doped N-enriched hollow carbon as efficient electrocatalyst for oxygen reduction reaction. *Chem. Eng. J.* **2020**, *397*, 125539. [[CrossRef](#)]
32. Li, L.; Dai, P.; Gu, X.; Wang, Y.; Yan, L.; Zhao, X. High oxygen reduction activity on a metal-organic framework derived carbon combined with high degree of graphitization and pyridinic-N dopants. *J. Mater. Chem. A Mater.* **2017**, *5*, 789–795. [[CrossRef](#)]
33. Jin, M.; Lu, S.-Y.; Zhong, X.; Liu, H.; Liu, H.; Gan, M.; Ma, L. Spindle-Like MOF Derived TiO<sub>2</sub>@NC-NCNTs Composite with Modulating Defect Site and Graphitization Nanoconfined Pt NPs as Superior Bifunctional Fuel Cell Electrocatalysts. *ACS Sustain. Chem. Eng.* **2020**, *8*, 1933–1942. [[CrossRef](#)]
34. Guo, Y.; Dong, A.; Huang, Q.; Li, Q.; Hu, Y.; Qian, J.; Huang, S. Hierarchical N-doped C.N.T.s grafted onto MOF-derived porous carbon nanomaterials for efficient oxygen reduction. *J. Colloid Interface Sci.* **2022**, *606*, 1833–1841. [[CrossRef](#)]
35. Rong, J.; Gao, E.; Liu, N.; Chen, W.; Rong, X.; Zhang, Y.; Zheng, X.; Ao, H.; Xue, S.; Huang, B.; et al. Porphyrinic MOF-derived rich N-doped porous carbon with highly active CoN<sub>4</sub>C single-atom sites for enhanced oxygen reduction reaction and Zn-air batteries performance. *Energy Storage Mater.* **2023**, *56*, 165–173. [[CrossRef](#)]
36. Chen, X.; Wang, N.; Shen, K.; Xie, Y.; Tan, Y.; Li, Y. MOF-Derived Isolated Fe Atoms Implanted in N-Doped 3D Hierarchical Carbon as an Efficient ORR Electrocatalyst in Both Alkaline and Acidic Media. *ACS Appl. Mater. Interfaces* **2019**, *11*, 25976–25985. [[CrossRef](#)]
37. Lu, X.; Wu, M.; Lu, Z.; Hu, J.; Xie, J.; Hao, A.; Cao, Y. Construction of multiple active sites by solution-free self-generating dual-template strategy: Boosting the ORR performance of NiFe/N-doped 3D porous carbon nanosheets. *J. Alloys Compd.* **2023**, *942*, 169095. [[CrossRef](#)]
38. Li, J.; Xia, W.; Tang, J.; Tan, H.; Wang, J.; Kaneti, Y.V.; Bando, Y.; Wang, T.; He, J.; Yamauchi, Y. MOF nanoleaves as new sacrificial templates for the fabrication of nanoporous Co-N:X/C electrocatalysts for oxygen reduction. *Nanoscale Horiz.* **2019**, *4*, 1006–1013. [[CrossRef](#)]
39. Siburian, R.; Kondo, T.; Nakamura, J. Size Control to a Sub-Nanometer Scale in Platinum Catalysts on Graphene. *J. Phys. Chem. C* **2013**, *117*, 3635–3645. [[CrossRef](#)]
40. Xili, D.; Zhou, Q.; Zhang, L. Well-defined Co-N-C catalyst based on ZIF-67 in mixed solvents with low amount of ligands for efficient oxygen reduction reaction. *J. Alloys Compd.* **2022**, *911*, 165072. [[CrossRef](#)]
41. Zhang, H.; Hwang, S.; Wang, M.; Feng, Z.; Karakalos, S.; Luo, L.; Qiao, Z.; Xie, X.; Wang, C.; Su, D.; et al. Single Atomic Iron Catalysts for Oxygen Reduction in Acidic Media: Particle Size Control and Thermal Activation. *J. Am. Chem. Soc.* **2017**, *139*, 14143–14149. [[CrossRef](#)]
42. Zhong, L.; Li, S. Unconventional Oxygen Reduction Reaction Mechanism and Scaling Relation on Single-Atom Catalysts. *ACS Catal.* **2020**, *10*, 4313–4318. [[CrossRef](#)]
43. Ge, X.; Sumboja, A.; Wuu, D.; An, T.; Li, B.; Goh, F.W.T.; Hor, T.S.A.; Zong, Y.; Liu, Z. Oxygen Reduction in Alkaline Media: From Mechanisms to Recent Advances of Catalysts. *ACS Catal.* **2015**, *5*, 4643–4667. [[CrossRef](#)]

44. Chen, Z.; Higgins, D.; Yu, A.; Zhang, L.; Zhang, J. A review on non-precious metal electrocatalysts for PEM fuel cells. *Energy Environ. Sci.* **2011**, *4*, 3167–3192. [[CrossRef](#)]
45. Zhang, X.; Xue, D.; Jiang, S.; Xia, H.; Yang, Y.; Yan, W.; Hu, J.; Zhang, J. Rational confinement engineering of MOF-derived carbon-based electrocatalysts toward CO<sub>2</sub> reduction and O<sub>2</sub> reduction reactions. *InfoMat* **2022**, *4*, e12257. [[CrossRef](#)]
46. Kim, M.; Yi, J.; Park, S.H.; Park, S.S. Heterogenization of Molecular Electrocatalytic Active Sites through Reticular Chemistry. *Adv. Mater.* **2023**, *35*, 2203791. [[CrossRef](#)]
47. Yang, L.; Zeng, X.; Wang, W.; Cao, D. Recent Progress in MOF-Derived, Heteroatom-Doped Porous Carbons as Highly Efficient Electrocatalysts for Oxygen Reduction Reaction in Fuel Cells. *Adv. Funct. Mater.* **2018**, *28*, 1704537. [[CrossRef](#)]
48. Liu, Z.; Yan, P.; Bai, Y.; Zhang, Z.; Li, X.; Xiong, W.; Zhang, J.; Yuan, A.; Zheng, F. High synergetic transition metal phosphides@nitrogen doped porous carbon nanosheets hybrids derived from silk fibroin and phytic acid self-assembly for ultra-high performance lithium storage. *J. Alloys Compd.* **2022**, *920*, 165832. [[CrossRef](#)]
49. Song, Y.; Li, X.; Sun, L.; Wang, L. Metal/metal oxide nanostructures derived from metal-organic frameworks. *RSC Adv.* **2015**, *5*, 7267–7279. [[CrossRef](#)]
50. Yang, J.; Li, P.; Wang, L.; Guo, X.; Guo, J.; Liu, S. In-situ synthesis of Ni-MOF@CNT on graphene/Ni foam substrate as a novel self-supporting hybrid structure for all-solid-state supercapacitors with a high energy density. *J. Electroanal. Chem.* **2019**, *848*, 113301. [[CrossRef](#)]
51. Huang, H.; Shen, K.; Chen, F.; Li, Y. Metal-organic frameworks as a good platform for the fabrication of single-atom catalysts. *ACS Catal.* **2020**, *10*, 6579–6586. [[CrossRef](#)]
52. Zhou, L.; Zhou, P.; Zhang, Y.; Liu, B.; Gao, P.; Guo, S. 3D star-like atypical hybrid MOF derived single-atom catalyst boosts oxygen reduction catalysis. *J. Energy Chem.* **2021**, *55*, 355–360. [[CrossRef](#)]
53. Ding, S.; Barr, J.A.; Shi, Q.; Zeng, Y.; Tieu, P.; Lyu, Z.; Fang, L.; Li, T.; Pan, X.; Beckman, S.P.; et al. Engineering Atomic Single Metal–FeN<sub>4</sub>Cl Sites with Enhanced Oxygen-Reduction Activity for High-Performance Proton Exchange Membrane Fuel Cells. *ACS Nano* **2022**, *16*, 15165–15174. [[CrossRef](#)]
54. Xie, X.; Shang, L.; Xiong, X.; Shi, R.; Zhang, T. Fe Single-Atom Catalysts on MOF-5 Derived Carbon for Efficient Oxygen Reduction Reaction in Proton Exchange Membrane Fuel Cells. *Adv. Energy Mater.* **2022**, *12*, 2102688. [[CrossRef](#)]
55. Li, J.; Xia, W.; Tang, J.; Gao, Y.; Jiang, C.; Jia, Y.; Chen, T.; Hou, Z.; Qi, R.; Jiang, D.; et al. Metal-Organic Framework-Derived Graphene Mesh: A Robust Scaffold for Highly Exposed Fe-N<sub>4</sub>Active Sites toward an Excellent Oxygen Reduction Catalyst in Acid Media. *J. Am. Chem. Soc.* **2022**, *144*, 9280–9291. [[CrossRef](#)]
56. Wang, K.; Chu, Y.; Zhang, X.; Zhao, R.; Tan, X. Facile Method to Synthesize a High-Activity S-Doped Fe/S.N.C. Single-Atom Catalyst by Metal–Organic Frameworks for Oxygen Reduction Reaction in Acidic Medium. *Energy Fuels* **2021**, *35*, 20243–20249. [[CrossRef](#)]
57. Anwar, S.; Khan, F.; Zhang, Y.; Djire, A. Recent development in electrocatalysts for hydrogen production through water electrolysis. *Int. J. Hydron. Energy* **2021**, *46*, 32284–32317. [[CrossRef](#)]
58. Deng, Y.; Chi, B.; Li, J.; Wang, G.; Zheng, L.; Shi, X.; Cui, Z.; Du, L.; Liao, S.; Zang, K.; et al. Atomic Fe-Doped MOF-Derived Carbon Polyhedrons with High Active-Center Density and Ultra-High Performance toward PEM Fuel Cells. *Adv. Energy Mater.* **2019**, *9*, 1802856. [[CrossRef](#)]
59. Wang, Z.; Meng, X.; Wang, H.; Bao, L.; Li, C.; Cong, Y.; Zhao, Q. MOF-derived carbon nanotubes as an highly active electrocatalyst for oxygen reduction reaction in alkaline and acidic media. *Int. J. Electrochem. Sci.* **2023**, *18*, 100131. [[CrossRef](#)]
60. Ali Khan, I.; Qian, Y.; Badshah, A.; Arif Nadeem, M.; Zhao, D. Highly Porous Carbon Derived from MOF-5 as a Support of ORR Electrocatalysts for Fuel Cells. *ACS Appl. Mater. Interfaces* **2016**, *8*, 17268–17275. [[CrossRef](#)]
61. Gamal, S.; Kospa, D.A.; Gebreil, A.; El-Hakam, S.A.; Ahmed, A.I.; Ibrahim, A.A. NiCo<sub>2</sub>O<sub>4</sub> spinel supported N-dopped porous Hollow carbon derived MOF functionalized SiO<sub>2</sub> for efficient ORR electrocatalysis. *Int. J. Hydron. Energy* **2023**, *48*, 18890–18905. [[CrossRef](#)]
62. Kuang, X.; Luo, Y.; Kuang, R.; Wang, Z.; Sun, X.; Zhang, Y.; Wei, Q. Metal organic framework nanofibers derived Co<sub>3</sub>O<sub>4</sub>-doped carbon-nitrogen nanosheet arrays for high efficiency electrocatalytic oxygen evolution. *Carbon* **2018**, *137*, 433–441. [[CrossRef](#)]
63. Niu, Y.; Yuan, Y.; Zhang, Q.; Chang, F.; Yang, L.; Chen, Z.; Bai, Z. Morphology-controlled synthesis of metal-organic frameworks derived lattice plane-altered iron oxide for efficient trifunctional electrocatalysts. *Nano Energy* **2021**, *82*, 105699. [[CrossRef](#)]
64. Xu, G.; Xu, G.-C.; Ban, J.-J.; Zhang, L.; Lin, H.; Qi, C.-L.; Sun, Z.-P.; Jia, D.-Z. Cobalt and cobalt oxides N-codoped porous carbon derived from metal-organic framework as bifunctional catalyst for oxygen reduction and oxygen evolution reactions. *J. Colloid Interface Sci.* **2018**, *521*, 141–149. [[CrossRef](#)] [[PubMed](#)]
65. Chen, C.; Tuo, Y.; Lu, Q.; Lu, H.; Zhang, S.; Zhou, Y.; Zhang, J.; Liu, Z.; Kang, Z.; Feng, X.; et al. Hierarchical trimetallic Co-Ni-Fe oxides derived from core-shell structured metal-organic frameworks for highly efficient oxygen evolution reaction. *Appl. Catal. B* **2021**, *287*, 119953. [[CrossRef](#)]
66. Sun, T.; Zhang, S.; Xu, L.; Wang, D.; Li, Y. An efficient multifunctional hybrid electrocatalyst: Ni<sub>2</sub>P nanoparticles on MOF-derived Co,N-doped porous carbon polyhedrons for oxygen reduction and water splitting. *Chem. Commun.* **2018**, *54*, 12101–12104. [[CrossRef](#)]
67. Li, L.; Xie, W.; Chen, J.; Yang, J. ZIF-67 derived P/Ni/Co/NC nanoparticles as highly efficient electrocatalyst for oxygen reduction reaction (ORR). *J. Solid State Chem.* **2018**, *264*, 1–5. [[CrossRef](#)]

68. Li, X.; Jiang, Q.; Dou, S.; Deng, L.; Huo, J.; Wang, S. ZIF-67-derived Co-NC@CoP-NC nanopolyhedra as an efficient bifunctional oxygen electrocatalyst. *J. Mater. Chem. A Mater.* **2016**, *4*, 15836–15840. [[CrossRef](#)]
69. Tang, B.; Wang, S.; Long, J. Novel in-situ P-doped metal-organic frameworks derived cobalt and heteroatoms co-doped carbon matrix as high-efficient electrocatalysts. *Int. J. Hydrot. Energy* **2020**, *45*, 32972–32983. [[CrossRef](#)]

**Disclaimer/Publisher’s Note:** The statements, opinions and data contained in all publications are solely those of the individual author(s) and contributor(s) and not of MDPI and/or the editor(s). MDPI and/or the editor(s) disclaim responsibility for any injury to people or property resulting from any ideas, methods, instructions or products referred to in the content.